

fMRI resting state networks define distinct modes of long-distance interactions in the human brain

M. De Luca,^{a,b,*} C.F. Beckmann,^a N. De Stefano,^b P.M. Matthews,^a and S.M. Smith^a

^aOxford Centre for Functional Magnetic Resonance Imaging of the Brain, UK

^bInstitute of Neurological Science, University of Siena, Italy

Received 26 May 2005; revised 16 August 2005; accepted 25 August 2005
Available online 2 November 2005

Functional magnetic resonance imaging (fMRI) studies of the human brain have suggested that low-frequency fluctuations in resting fMRI data collected using blood oxygen level dependent (BOLD) contrast correspond to functionally relevant resting state networks (RSNs). Whether the fluctuations of resting fMRI signal in RSNs are a direct consequence of neocortical neuronal activity or are low-frequency artifacts due to other physiological processes (e.g., autonomically driven fluctuations in cerebral blood flow) is uncertain. In order to investigate further these fluctuations, we have characterized their spatial and temporal properties using probabilistic independent component analysis (PICA), a robust approach to RSN identification. Here, we provide evidence that: i. RSNs are not caused by signal artifacts due to low sampling rate (aliasing); ii. they are localized primarily to the cerebral cortex; iii. similar RSNs also can be identified in perfusion fMRI data; and iv. at least 5 distinct RSN patterns are reproducible across different subjects. The RSNs appear to reflect “default” interactions related to functional networks related to those recruited by specific types of cognitive processes. RSNs are a major source of non-modeled signal in BOLD fMRI data, so a full understanding of their dynamics will improve the interpretation of functional brain imaging studies more generally. Because RSNs reflect interactions in cognitively relevant functional networks, they offer a new approach to the characterization of state changes with pathology and the effects of drugs.

© 2005 Elsevier Inc. All rights reserved.

Keywords: Functional MRI; Brain activation; Resting state; Independent component analysis; Functional connectivity; Resting state networks; PICA; Perfusion fMRI

Introduction

The functioning of the human brain during rest can be investigated using different functional imaging techniques (Biswal et al., 1995; Shulman et al., 1997; Gusnard and Raichle, 2001). While the resting state is an ill-defined condition, consistent functional patterns across individuals should represent common “default” or “idling” state activity. Long-range coherences in these activities therefore could reflect strong functional connectivities.

fMRI images obtained using blood oxygen level dependent (BOLD) contrast show signal fluctuations at rest. These fluctuations occur at low frequencies (0.01–0.05 Hz) and have been shown to be coherent across widely separated (although functionally related) brain regions (e.g., bihemispheric sensorimotor cortices) (Biswal et al., 1995; Lowe et al., 1998; Cordes et al., 2000). Regions showing coherent fluctuations therefore constitute a “resting state network” (RSN). We and others have appreciated that there is more than one spatially distinct RSN in a resting brain image dataset, with each RSN having a distinct signal time-course (De Luca et al., 2002; Greicius et al., 2003).

Whether the fluctuations of resting fMRI signal in RSNs are a direct consequence of neuronal activity or whether they reflect phenomena such as cardio-respiratory motion or vascular modulation is uncertain. The normally low sampling rate of fMRI images (Jezzard et al., 2002) causes temporal aliasing of variations of the BOLD fMRI signal induced by cardiac and respiratory cycles into a low-frequency range, similar to that of the RSN signal fluctuations. Some low-frequency coherences in resting BOLD fMRI data are clearly a consequence of this physiological noise (Lowe et al., 1998; Xiong et al., 1999; Cordes et al., 2000). However, studies conducted in ways that avoid aliasing of the fMRI signal (using a fast image sampling rate) show that many low-frequency coherences are still present, suggesting that RSNs and (higher frequency) physiological noise are phenomenologically distinct processes (Biswal et al., 1995; Lowe et al., 1998). Additional patterns related directly to vascular processes independent of cortical neuronal function have been identified as low-frequency fluctuations in resting fMRI data (Kiviniemi et al., 2000; Wise et al., 2004). The most direct data relating some patterns of

* Corresponding author. FMRIB Centre, University of Oxford, John Radcliffe Hospital, Headley Way, Headington, Oxford OX3 9DU, UK. Fax: +44 1865 222717.

E-mail address: marilena@fmrib.ox.ac.uk (M. De Luca).

Available online on ScienceDirect (www.sciencedirect.com).

low-frequency coherence in fMRI data to neuronal activity come from evidence that the underlying fluctuations are correlated with modulations of cortical electrical activity detected by EEG (Goldman et al., 2002; Leopold et al., 2003; Moosmann et al., 2003; Laufs et al., 2003). The observation of changes in patterns with neurological disease (e.g., Alzheimer's disease; Greicius et al., 2004) is consistent with this.

An important concern in studying RSNs is whether the method used for their identification is appropriately sensitive, yet relatively unbiased. Methods based on direct correlations with time-courses of signal change identified from a “seed” voxel are limited to applications to regions for which there is an a priori expectation of a network pattern.

Here, we have applied probabilistic ICA (PICA) to the characterization of RSNs in resting brain BOLD contrast datasets. We have made a series of observations designed to test: i. the independence of PICA-defined RSNs from artifacts related to cardio-respiratory motion; ii. the localization of potential generators of RSNs; iii. the relation of BOLD RSNs to coherences defined with perfusion imaging; iv. the reproducibility of RSNs across subjects; and v. the specific patterns of coherent activity across the brain.

Methods

All fMRI data were acquired from healthy volunteers (age range 22–51 years). In all experiments, subjects were at rest; they were instructed to relax with their eyes closed, without falling asleep, as confirmed by the subjects after completion of the experiment. MRI data were acquired on a 3 T Varian/Siemens MRI system at the Oxford Centre for Functional Magnetic Imaging of the Brain, except the data of experiment 1, which were collected on a 1.5 T Philips Gyroscan MRI system at the NMR Centre of the University of Siena. Temporal and spatial resolutions of fMRI data varied across the experiments; they are detailed in the following sections.

All data were first pre-processed using tools from the FMRIB Software Library (FSL, <http://www.fmrib.ox.ac.uk/fsl>) (Smith et al., 2004), applying the following procedures: motion correction (Jenkinson et al., 2002), spatial smoothing using a Gaussian kernel of FWHM 5 mm, mean-based intensity normalization of all volumes by the same factor, and high-pass temporal filtering (Gaussian-weighted least-squares straight line fitting, with high-pass filter cut-off of 250s). Following the pre-processing, the data were analyzed using MELODIC (Multivariate Exploratory Linear Optimised Decomposition into Independent Components), an implementation of probabilistic independent component analysis (PICA) (Beckmann and Smith, 2004), also part of FSL.

Independent component analysis (ICA) is becoming a popular exploratory method for analyzing complex data such as that from fMRI experiments. ICA views the 4D data as a sum of a set of spatiotemporal components, each of which consists of a spatial map modulated in time by that component's associated time-

course. It attempts to separate the different components by making the assumption that the spatial maps are statistically independent of each other, and, having different time-courses, they will ideally each represent a different artefact or activation pattern. By using the entire 4D dataset at once in this multivariate analysis, this kind of approach does not need to be fed any temporal model. In attempting to find RSNs in fMRI data, it is preferable to use a methodology that does not require the additional experimental sessions, extra analysis steps, and potential bias associated with activation-derived seeding.

The application of “model-free” methods such as ICA, however, has previously been restricted both by the view that results can be hard to interpret, and by the lack of ability to quantify statistical significance for estimated spatial maps. Beckmann and Smith (2004) proposed a probabilistic ICA (PICA) model for fMRI which models the observations as mixtures of spatially non-Gaussian signals and artefacts *in the presence of Gaussian noise*. It was demonstrated in the same work that using an objective estimation of the amount of Gaussian noise through Bayesian analysis of the number of activation and (non-Gaussian) noise sources, the problem of overfitting can be overcome. The approach proposed for estimating a suitable model order (i.e., how many ICA components to find) also allows for a unique decomposition of the data and reduces problems of interpretation as each final component is more likely to be due to only one physical or physiological process.

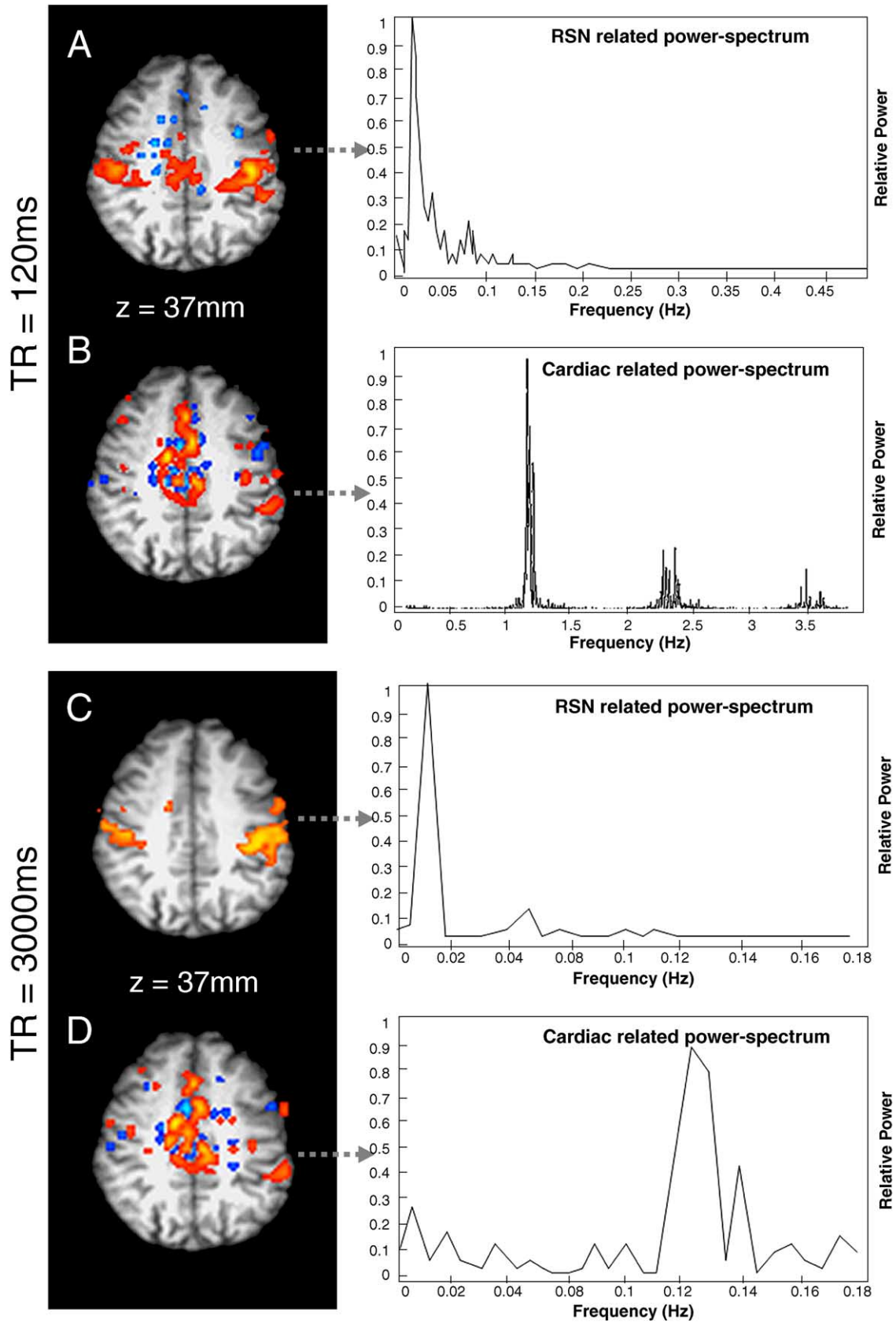
Experiment 1

The objective of this experiment was to assess if aliasing of physiological processes (cardiac and respiratory cycles) is distinguishable from “true” RSNs observed in fMRI data. The cardiac and respiratory cycles occur around 1 Hz and 0.3 Hz respectively. Consequently, these can become aliased at typical TRs (2–3 s), giving significant power at the frequencies typical of RSNs. Because at low TRs (below 125 ms) such aliasing is avoided, in this experiment, BOLD fMRI data were collected using a very short TR (120 ms); see also Lowe et al. (1998). In addition, longer TR (3 s) BOLD fMRI data were collected and compared to the results from the low TR data. This was in order to test (via spatial comparison of PICA components) whether RSN signal is distinct (and distinguishable) from aliased signal changes related to the cardiac or respiratory cycles.

Two BOLD echo planar imaging fMRI datasets were collected from a single subject at 3 T, with the following parameters. In the first dataset (long TR), three axial slices covering the motor cortex (in-plane resolution 3.75×3.75 mm, slice thickness 7 mm, no gap, TR = 3000 ms, TE = 30 ms, 200 volumes) were collected during bilateral finger tapping (30s ON–OFF paradigm). In the second dataset (short TR), one single slice covering the motor cortex (in-plane resolution 3.75×3.75 mm, slice thickness 7 mm, TR = 120 ms, TE = 30 ms, 2200 volumes) was collected during rest.

The comparison of the maps obtained from the two experiments was performed by means of spatial correlation coefficients. In

Fig. 1. Resting state networks and the aliasing problem. (A and B) BOLD fMRI data collected with high temporal resolution (TR = 120 ms). Spatial distribution of probabilistic independent components and their relative power spectra respectively for (A) a resting state network in the motor cortex and (B) cardiac fluctuation (with harmonics). PICA separates the physiological noise induced by the cardiac cycle from the RSN. (C and D) BOLD fMRI data collected with low (more typical) temporal resolution (TR = 3000 ms). Spatial distribution of probabilistic independent components and their relative power spectra for resting state networks (C) and aliased cardiac-related artifact (D). PICA can separate the aliased physiological noise induced by the cardiac cycle from the RSN. All the maps are thresholded with alternative hypothesis, $P > 0.5$.



addition, an estimation of the aliased frequency, at different TRs, of the fundamental frequency, was also carried out for the cardiac and respiratory cycle.

Experiment 2

The objective of this experiment was to address the issue of spatial localization of RSNs, specifically their localization with respect to gray matter localization. BOLD fMRI images with relatively high spatial resolution, compared to a typical fMRI resolution (such as $4 \times 4 \times 7$ mm), were collected to investigate whether RSNs are localized within gray matter.

Two BOLD fMRI datasets were collected from two subjects at 3 T during rest. In the first subject, the following parameters were employed: 12 axial slices, in-plane resolution 2×2 mm, slice thickness 6 mm, no gap, TR = 3000 ms, TE = 40 ms, 300 volumes. In the second subject, the following parameters were employed: 30 axial slices, in-plane resolution 2×1.5 mm, slice thickness 1.75 mm, no gap, TR = 10 s, TE = 40 ms, 200 volumes. The parameters were optimized to achieve high spatial resolution and are different in the two subjects as we varied the balance between resolution and signal-to-noise in the two cases.

Experiment 3

More than one mechanism could contribute to the origin of these signals. If low-frequency coherences localized to gray matter arise from neuronal activity, then we hypothesize that they should also be reflected as local increases in blood flow. To test for such coherences specifically in *cerebral blood flow* changes across the brain, arterial spin-labeling perfusion imaging was used to acquire serial images of the resting brain.

For this purpose, we acquired resting ASL (arterial spin labeling) perfusion fMRI data (Kwong et al., 1992; Biswal et al., 1997). The ASL contrast mechanism is purely sensitive to blood flow, as opposed to BOLD fMRI, which is also sensitive to local oxygenation. Three perfusion fMRI datasets were collected from one single subject at rest, with the following parameters: 5 axial slices (totaling 15 slices covering whole brain), in-plane resolution 4×4 mm, slice thickness 6 mm, no gap, TR = 2000 ms, TE = 20 ms, TI = 1400 ms, 200 volumes. Previously, an RSN in the motor cortex was found in ASL data using a seeding approach (Biswal et al., 1997). As with the BOLD contrast, we applied PICA to the resting ASL data to define spatiotemporal networks, enabling us to look for multiple independent RSNs (if present) without the need for prespecification of the number of RSNs expected or selection of a seed voxel.

Experiment 4

The objective of this experiment was to investigate the spatial reproducibility of the RSNs across different subjects. Spatial reproducibility was assessed through spatial correlation of the RSN maps. Whole-brain BOLD fMRI datasets were collected from 10 subjects at 3 T, during rest, using the following parameters: 45 axial slices, in-plane resolution 3×3 mm, slice thickness 3 mm, no gap, TR = 3400 ms, TE = 40 ms, 200 volumes.

After the separate single-subject PICA analyses, in order to combine the results from different subjects, RSN maps were first

aligned to the subjects' structural images and then into a standard (MNI152) space. They were then smoothed using a 5 mm FWHM Gaussian kernel. This was carried out to reduce the effect of structural differences between subjects (i.e. equivalent to the smoothing often applied in standard multi-subject fMRI experiments) (Jezzard et al., 2002, Chapter 14).

Spatial consistency between different RSN maps was quantified by finding the (spatial) normalized correlation coefficient of each map from one subject with each map of another subject. The correlations were thresholded at 0.15, corresponding to a probability level $P < 0.00015$.

RSN maps that were spatially consistent across all subjects were detected by looking for consistent sets of pair-wise correlations between all subjects (in all the directions). In other words, let us suppose we had only three subjects. If map j of group 1 (where group indicates the set of maps obtained from a PICA decomposition of one subject's data) was correlated with map i of group 2 and with map k of group 3, in order to declare these maps consistent, we had to verify that map k was also correlated with map j . This was not always true since we were dealing with thresholded correlation coefficients.

After identifying spatial maps that are consistent across subjects, we then created group maps using a fixed-effects analysis. For inference, we then ran mixture-modeling (alternative hypothesis testing, thresholded at $P > 0.5$ for "activation" vs. null (Beckmann and Smith, 2004) to create the thresholded results for each group-level RSN.

Finally, we tested whether diffusion-derived anatomical (white matter) connectivity supports the found networks. We used a probabilistic representation of thalamic nuclei derived from diffusion tensor data (Johansen-Berg et al., 2005, <http://www.fmrib.ox.ac.uk/connect>) to test whether RSN peaks lying in the thalamus were both functionally connected to particular cortical areas in the RSN maps (i.e., part of the same RSN) and anatomically connected in the diffusion atlas to these same cortical areas.

Results

Characterization of spatiotemporally distinct patterns of coherent signals in BOLD and ASL images from the unstimulated brain: resting state networks

PICA applied to a time series of echo planar brain images acquired from a subject at rest using either typical (3 s) or short (0.12 s) TR generates a series of spatiotemporally distinct patterns of coherent signal changes defined by BOLD fMRI (Fig. 1). Coherent RSN patterns can be identified having most power at very low frequencies (0.01–0.05 Hz, Figs. 1A, C). These are spatially very similar at both long and typical TR (compare also with Figs. 3–5) and are also temporally very similar and having the characteristic power spectrum of RSNs. A cardiac-related component can be clearly seen in Fig. 1B, where the (temporal) power spectrum peaks at the expected frequency of approximately 1 Hz. The associated spatial map has very strong similarity to Fig. 1D—suggesting that PICA has successfully identified the cardiac component even in the typical TR (where the time-course is aliased, as can be seen in the power spectrum of Fig. 1D) and successfully separated the RSN from the cardiac component. In these datasets, the only robust physiological components found

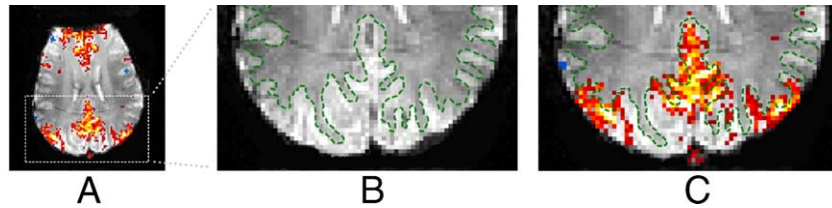


Fig. 2. Cortical localization of resting state networks. In relatively high-resolution BOLD fMRI datasets (in-plane resolution of 2×2 mm), RSN components are localized in cortical gray matter. The green lines represent the gray–white matter border in the selected area, after manually segmenting the image.

were the RSNs and the cardiac pulsation—that is, we did not find strong signal relating to respiration.

The apparent anatomical co-localization of low-frequency RSN coherences with gray matter were confirmed using higher-resolution fMRI. In both higher-resolution datasets, patterns were seen which corresponded (spatially) very well with the more typical resolutions acquired. For example, Fig. 2 shows an RSN spatial component resulting from PICA applied to the 2×2 mm in-plane resolution data. This has clear spatial similarity to the maps shown in Figs. 4 and 5, and it can be seen that the voxels involved in the RSN do indeed lie within gray matter. The $2 \times 1.5 \times 1.75$ mm data gave a similar general spatial pattern, but the greatly reduced voxel size in this dataset resulted in much noisier and less interpretable results.

The ASL perfusion data showed low-frequency coherences in a pattern similar to that found with BOLD contrast (Fig. 3). PICA performed on perfusion fMRI resting data disclosed five independent component (ICs) whose spatial and temporal characteristics strongly matched the RSNs observed in BOLD fMRI resting data (compare with Figs. 4 and 5).

Resting state networks are found consistently across subjects and define functional–anatomically related regions in the brain

If RSNs define “default” states of coherent activity across the brain, then they should be reproducible between healthy, alert individuals. The number of components extracted by ICA from

each subject varied from 42 to 67. This included scanner-related artefacts such as EPI ghosting and physiological artefacts such as cardiac pulsation. Spatial cross-correlation showed that a consistent set of five spatiotemporally distinct patterns was identified for all 10 subjects studied. Fig. 4 illustrates the five RSNs found with a typical single subject’s dataset.

To understand the anatomical relations of these resting fluctuations, the 5 spatiotemporally distinct RSNs from the 10 different subjects were registered individually into common brain space maps using PICA. The resulting group average RSN maps confirmed defined distinct patterns for each network (Fig. 5). Co-representation of the group average networks together emphasizes the complementary patterns of activation.

The coordinates of maxima in each activation cluster defined in the group maps were used to localize functional–anatomical regions attributed to the RSN. Individual RSNs then were classified spatially both on the basis of coordinates in standard space (Table 1) and by regional anatomy:

1. RSN1: a posterior network characterized by involvement predominantly of occipital cortex, as well as temporal–parietal regions;
2. RSN2: a posterior–lateral and midline network involving primarily the precuneus and anterior pole of the prefrontal lobe, as well as parietal regions.
3. RSN3: a lateral and midline network including the pre- and post-central gyri, as well as midline regions including the thalamus and hippocampus.

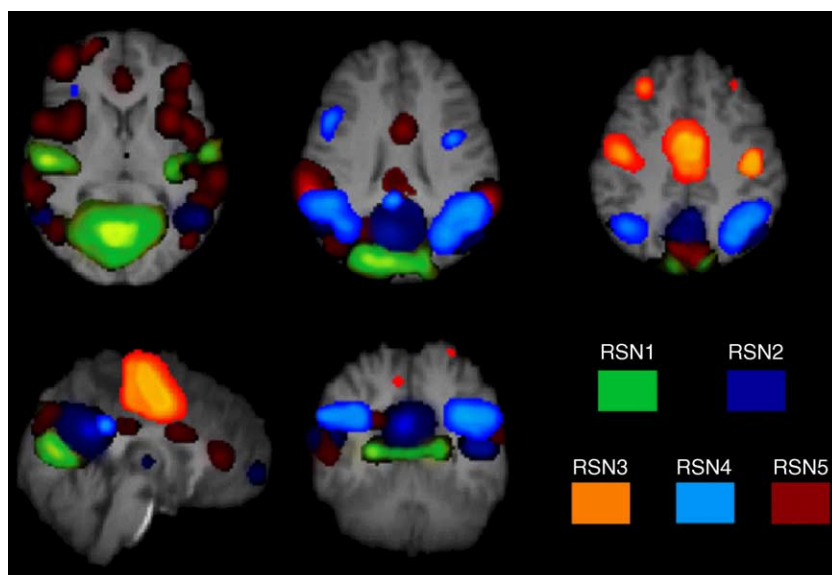


Fig. 3. Resting state networks are identifiable in perfusion fMRI data. PICA performed on perfusion fMRI resting data disclosed five independent component (ICs) whose spatial and temporal characteristics strongly matched the RSNs observed in BOLD fMRI resting data (compare with Fig. 5).

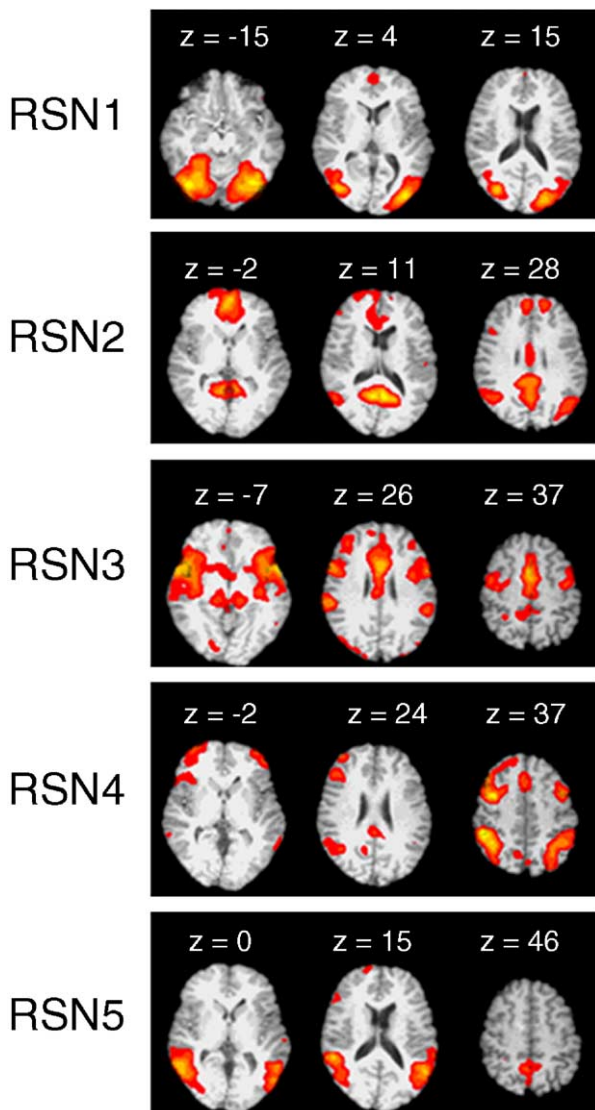


Fig. 4. Consistently identified resting state networks. Five RSNs from a single subject illustrating those found consistently from all subjects are shown. Maps are thresholded at $P > 0.5$ (alternative hypothesis threshold, for activation versus null). Each row represents the three most interesting slices of one distinct RSN. The RSNs are shown on the corresponding structural image transformed into standard space.

4. RSN4: a network involving dorsal parietal and predominantly lateral prefrontal cortex.
5. RSN5: a ventral network dominated by coherences between the inferior occipital parietal, temporal, and inferior prefrontal cortices.

Using the coordinates in Table 1, we were able to test more specifically the relationship between the anatomy of signal correlations defined in the RSNs and anatomical connectivity based on our prior definition of thalamo-cortical pathways using diffusion tensor imaging (Johansen-Berg et al., 2005). Using a probabilistic representation of the normal human thalamus defined on the basis of white matter connectivity to cortical regions, the anatomical relations between the thalamic activation cluster in RSNs 2 and 3 (Fig. 6) and the cortical regions were explored. The thalamic peak of coherence from the group RSN2 map corresponds to a region in the probabilistic thalamic atlas (Johansen-Berg et al., 2005, [\[www.fmrib.ox.ac.uk/connect\]\(http://www.fmrib.ox.ac.uk/connect\)\) with strongest connectivity to the prefrontal cortex, the localization of the correlated prefrontal activity in this RSN. By contrast, the anatomical localization of the thalamic cluster in RSN3 \(Fig. 6\) corresponds to a region that connects most anatomically strongly with motor cortex. Together, these results are consistent with a correspondence between regions showing RSN coherence and those with strong anatomical connectivities.](http://</p>
</div>
<div data-bbox=)

Discussion

Several previous reports have described specific patterns of low-frequency coherent signal in time series of gradient echo MRI from unstimulated brain (the brain “at rest”). The most commonly recognized pattern includes particularly the sensorimotor cortex bilaterally (corresponding to RSN 3 defined here) (Biswal et al.,

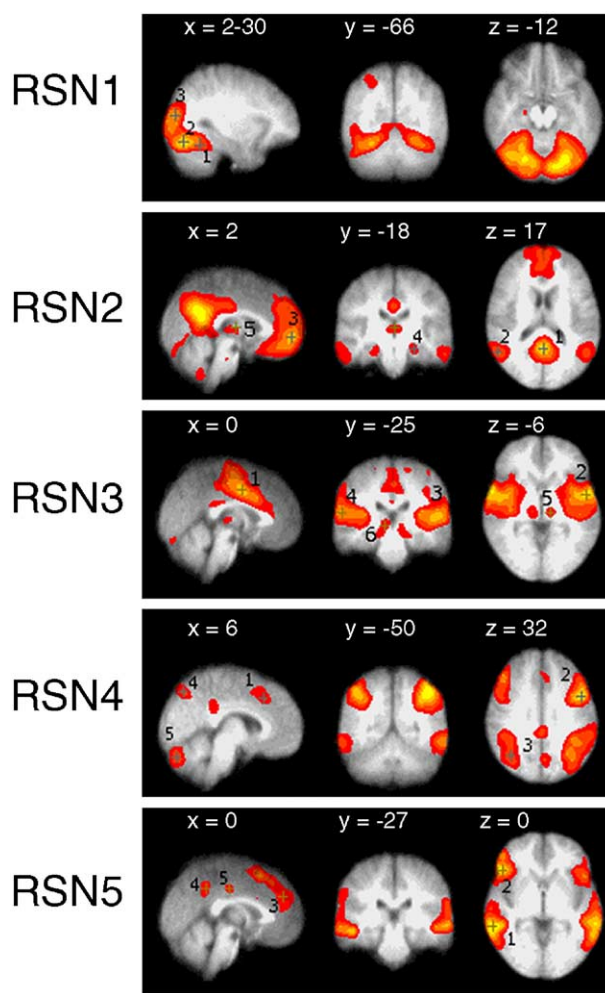


Fig. 5. Group resting state network maps. From top to bottom: (1) RSN 1 including visual cortical areas. The RSN reported here includes the main visual functional network. (2) RSN 2 including visuospatial and executive system. The RSN reported here includes the emotion/visuospatial processing functional network. (3) RSN 3 including sensory and auditory system. (4) RSN 4 including the dorsal pathway. (5) RSN 5 including ventral pathway. The crosses indicate the positions of the centers of the major clusters, and the corresponding coordinates are reported in Table 1 for each corresponding map (map obtained with alternative hypothesis threshold $P > 0.5$).

Table 1
Coordinates of the major clusters of the RSNs, as shown in Fig. 5 (cross points) in stereotactic space of Talairach and Tournoux (1988)

	Cluster	<i>x</i>	<i>y</i>	<i>z</i>	Anatomical region
RSN 1	1	6	-78	-3	BA18 Lingual gyrus
	2	24	-78	-10	BA18 Lingual gyrus
	3	-30	-89	20	BA19 Middle occipital gyrus
RSN 2	1	-2	-51	27	BA31 Cingulate gyrus
	2	53	-57	23	BA39 Superior temporal gyrus
	3	2	54	-3	BA10 Medial frontal gyrus
	4	-20	-19	-18	Hippocampus
	5	6	-19	6	Thalamus
RSN 3	1	-4	-6	40	BA24 Cingulate gyrus
	2	-51	-7	8	BA6 Precentral gyrus
	3	-55	-18	8	BA41 Superior temporal gyrus
	4	57	-5	20	BA4 Precentral gyrus
	5	12	-17	0	Thalamus
	6	22	-16	-13	Hippocampus
RSN 4	1	-2	-21	43	BA31 Paracentral lobule
	2	46	6	34	BA9 Middle frontal gyrus
	3	44	-48	46	BA40 Inferior parietal lobule
	4	-38	-56	48	BA7 Superior parietal lobule
	5	-55	-58	-9	BA37 Inferior temporal gyrus
RSN5	1	62	-37	-3	BA21 Middle temporal gyrus
	2	52	26	-4	BA47 Inferior frontal gyrus
	3	6	46	18	BA9 Medial frontal gyrus
	4	8	-46	41	BA31 Cingulate gyrus
	5	8	-16	40	BA24 Cingulate gyrus

Brain regions are identified by putative Brodmann area (BA).

1995; Lowe et al., 1998; Xiong et al., 1999). Other work characterized a predominantly occipital network (corresponding to RSN1 here) (Goldman and Cohen, 2003; Moosmann et al., 2003). Our study extends this description, using a relatively unbiased approach to analysis based on probabilistic ICA (Beckmann and Smith, 2004). We have identified 5 spatiotemporally distinct patterns of low-frequency coherences across the brain. The PICA method clearly distinguishes these patterns of activity from those associated with cardio-respiratory motion of the brain, even without sampling that is rapid with respect to the primary frequencies of these processes. We additionally have provided evidence for cortical localization of these coherences and for similar patterns associated with changes in local blood flow, consistent with the neuronal origin of the signals.

Our analysis using PICA found multiple patterns of coherence involving distinct functional-anatomical networks across the brain. While the coordinated neuronal activity that we infer is reflected in these hemodynamic changes *may* have a specific processing function, at this point, any such functions are unclear. Instead, therefore, we interpret the coherences more generally as indicative of “default” or “idling” mode of interactions between functionally integrated regions. As such, the coherences provide

insight into the dynamic functional architecture of the brain in the absence of activity coordinated for a specific task.

Previous work has provided evidence that some RSNs are correlated with slow modulations of EEG-measured neuronal activity in the *alpha* band (Goldman and Cohen, 2003; Goldman et al., 2002; Laufs et al., 2003) and *mu* band (Moosmann et al., 2003). Changes in the strengths of some coherences have been reported with neurological diseases (Greicius et al., 2004). Note that, while Goldman showed alpha-related changes in (our) RSNs 1 and 3, Laufs’ results appear spatially more similar to (our) RSNs 4 and 5. Therefore, though we can conclude that there does seem to be a strong correlation between the RSN time-courses and modulation of the alpha EEG component, much remains to be understood as to the exact nature of this link.

The PICA approach offers specific advantages relative to correlation-based analysis with “seeding” of a region identified by a prior stimulus activation study. The latter limits analysis to coherences specifically searched for. While the PICA method cannot be ideally sensitive to *all* such longer-range coherences, our results emphasize the potential richness of the time series data and the substantial extent of long-range coherences in fMRI datasets. A second limitation of the seeding approach is that it assumes that RSN coherences are related directly to regions identified by arbitrarily chosen types of activation. The strongest resting coherences may not be localized to the specific regions of functional cortex probed. For example, the low-frequency coherences between regions of sensorimotor cortex identified here were not maximal in the motor cortex hand regions previously used as seeds for correlation analysis. Thus, methodological differences potentially account for the more extensive patterns of activation implicated in RSNs reported here, as well as for the increased number of distinct patterns of coherent activity that we have identified. Reassuringly, where comparable regions are explored, results from correlation in PICA (or other ICA methods) are generally consistent (Greicius et al., 2004; De Luca et al., in press).

The reproducibility of patterns of coherence across the brain was explored directly in our study. Reproducibility of patterns between the individuals was good. There is some evidence that prior experience (e.g., training on a specific task) may modulate the relative strengths of coherences (Waites et al., 2005), though it is

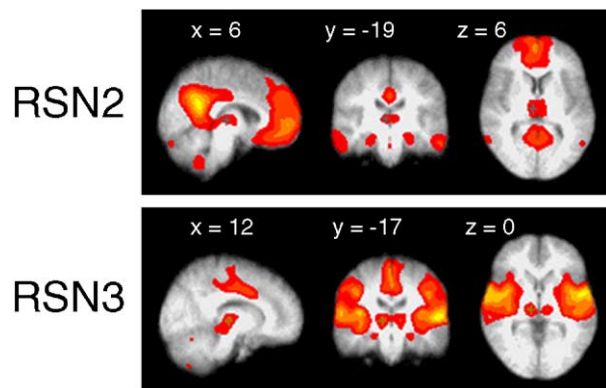


Fig. 6. RSN and thalamic connectivity. Top: the cross indicates the voxel in RSN 2 ($x = 6, y = -19, z = 6$ in MNI space) used for seeding an anatomical connectivity investigation, using a standard-space anatomical thalamus connectivity atlas. Bottom: the cross indicates the seeding voxel in RSN 3 ($x = 12, y = -17, z = 0$ in MNI space). A distinct pattern of anatomical connectivity is associated with the different resting state coherence.

clear from our data that, while such modulation can occur, the RSNs are quite robustly found across subjects. It remains to be seen whether RSNs can provide useful clinical or cognitive markers in the absence of an experimental task.

The ability to differentiate physiological noise variations from different sources is inherent to multivariate decomposition techniques such as PICA. In addition to signal changes that are potentially neurally mediated and those related to cardio-respiratory cycles, coherences can be found that appear more specifically localized to regions with large draining veins and may represent changes associated with either cerebral blood volume modulation or gross vessel movements (Kiviniemi et al., 2000). Instrument-related artefacts also can be identified (Beckmann and Smith, 2004).

The group-level RSNs identified relate to functional–anatomically distinct systems. RSN1 includes the striate and extra-striate cortex, regions involved in visual processing (Haxby et al., 1994). The relationship to slow modulation of alpha wave activity previously described suggests that this RSN could be modulated by levels of alertness, although this has not yet been demonstrated. RSN2, which involves the precuneus, anterior pole, and midline structures including the thalamus and hypothalamus, as well as medial parietal cortex, is closely related to patterns described as “deactivated” during active tasks in PET cerebral blood flow studies (Shulman et al., 1997; Mazoyer et al., 2001). These regions have been suggested to be associated in a functional network related to internal monitoring and states of consciousness (Gusnard and Raichle, 2001). RSN3 involves the post-central gyrus, insula, and midline cingulate in superior frontal gyrus. These regions are involved in motor control and somatosensation (Hsieh et al., 1999), suggesting that the network reflects functional and anatomical interactions relevant to the control of action. RSN4 includes occipital, dorsal, parietal, and prefrontal regions. Parietal and prefrontal regions are closely functionally integrated in a wide range of cognitive processes. The pattern here may recall more specifically the network of brain regions implicated in visual perception for action, the so-called “where” pathway (Ungerleider and Haxby, 1994). RSN5, by contrast, involves predominantly more inferior regions of occipital, parietal, and prefrontal cortex in a pattern recalling the complementary visual perceptual “what” pathway (Ungerleider and Haxby, 1994).

The agreement of RSN spatial localization and anatomical connectivity suggests that RSNs follow similar spatial organization to that inferred from DTI anatomical connectivity.

In summary, our analysis with PICA has identified several independently varying patterns of signal coherence across the brain in resting state BOLD fMRI. Similar patterns were shown to be able to be found with the more specific measure of hemodynamic response provided by perfusion imaging. The cortical localization of the generators and the similarity of the patterns to known functional–anatomical networks suggest that these arise with long-range coherences in neuronal activity. Although the interactions may have independent functional roles, these are not yet apparent. Their association with the unstimulated or “resting” brain suggests that they arise from “default” or “idling” state of these functional networks. They could thus simply represent a form of “noise” distributed across the networks as a consequence of their functional connectivity. Even in this instance, however, they potentially provide information on functional systems and the dynamics of interactions within them. They also may prove to be a useful probe for functional alterations in the brain as a consequence of changes in brain state, disease, or pharmacological interventions.

Acknowledgments

We are grateful to Dr. Giandomenico Iannetti and Dr. Joe Devlin for helpful discussion on RSN neuroscience meaning. We are grateful for financial support from the European PhD program, the UK Medical Research Council, the UK Engineering and Physical Sciences Research Council, and GlaxoSmithKline. We are grateful to S. Clare for the high spatial resolution data, M. Lowe for the low TR data, and to P. Chiarelli for the ASL data.

References

- Beckmann, C., Smith, S.M., 2004. Probabilistic independent component analysis for functional magnetic resonance imaging. *IEEE Trans. Med. Imag.* 23, 137–152.
- Biswal, B., Yetkin, F.Z., Haughton, V.M., Hyde, J.S., 1995. Functional connectivity in the motor cortex of resting human brain using echo-planar MRI. *J. Magn. Reson. Med.* 34, 537–541.
- Biswal, B., Kylen, J.V., Hyde, J.S., 1997. Simultaneous assessment of flow and bold signals in resting-state functional connectivity maps. *NMR Biomed.* 10, 165–170.
- Cordes, D., Haughton, V.M., Arfanakis, K., Wendt, G.J., Tursky, P.A., Moritzk, C.H., Quigley, M.A., Meyerand, M.E., 2000. Mapping functionally related regions of brain with functional connectivity MR imaging. *AJNR Am. J. Neuroradiol.* 21, 1636–1644.
- De Luca, M., Beckmann, C.F., Behrens, T., Clare, S., Matthews, P., De Stefano, N., Woolrich, M., Smith, S.M., 2002. Low frequency signals in fMRI—“resting state networks” and the “intensity normalisation problem”. *Proc. Int. Soc. of Magnetic Resonance in Medicine*.
- De Luca, M., Smith, S., De Stefano, N., Federico, A., Matthews, P.M., in press. BOLD contrast resting state networks are relevant to functional activity in the neocortical sensorimotor system. *Exp. Brain Res.*
- Goldman, R.I., Cohen, M., 2003. Tomographic distribution of resting alpha rhythm sources revealed by independent component analysis. *Ninth Int. Conf. on Functional Mapping of the Human Brain*.
- Goldman, R.I., Stern, J.M., Engel Jr., J., Cohen, M.S., 2002. Simultaneous EEG and fMRI of the alpha rhythm. *NeuroReport* 13 (18), 2487–2492 (Edition, 13 (18)).
- Greicius, M.D., Krasnow, B., Reiss, A.L., Menon, V., 2003. Functional connectivity in the resting brain: a network analysis of the default mode hypothesis. *Proc. Natl. Acad. Sci. U. S. A.*, 253–258.
- Greicius, M.D., Srivastava, G., Reiss, A.L., Menon, V., 2004. Default-mode network activity distinguishes Alzheimer’s disease from healthy aging: evidence from functional MRI. *Proc. Natl. Acad. Sci. U. S. A.*, 4637–4642.
- Gusnard, D.A., Raichle, M.E., 2001. Searching for a baseline: functional imaging and the resting human brain. *Nat. Rev., Neurosci.* 2, 685–692.
- Haxby, J.V., Horwitz, B., Ungerleider, L.G., Maisog, J.M., Pietrini, P., Grady, C.L., 1994. The functional organization of human extrastriate cortex: a pet–rcbf study of selective attention to faces and locations. *J. Neurosci.* 14, 6336–6353.
- Hsieh, J.C., Meyerson, B.A., Ingvar, M., 1999. Pet study on central processing of pain in trigeminal neuropathy. *Eur. J. Pain* 3 (1), 51–65.
- Jenkinson, M., Bannister, P.R., Brady, J.M., Smith, S.M., 2002. Improved optimisation for the robust and accurate linear registration and motion correction of brain images. *NeuroImage* 17 (2), 825–841.
- Jezzard, P., Matthews, P.M., Smith, S.M., 2002. *Functional Magnetic Resonance Imaging: an Introduction to Methods*, J. Cogn. Neurosci., vol. 9. Oxford Univ. Press (Chap. 14–15).
- Johansen-Berg, H., Behrens, T.E.J., Sillery, E.L., Ciccarelli, O., Wheeler-Kingshott, C.A.M., Thompson, A.J., Smith, S.M., Matthews, P.M., 2005. Functional–anatomical validation and individual variation of diffusion tractography-based segmentation of the human thalamus. *Cereb. Cortex* 15, 31–39.

- Kiviniemi, V., Jauhainen, J., Tervonen, O., Paakko, E., Oikarinen, J., Vainionpaa, V., Rantala, H., Biswal, B., 2000. Slow vasomotor fluctuation in fMRI in anesthetized child brain. *J. Magn. Reson. Med.* 44, 373–378.
- Kwong, K.K., Belliveau, J.W., Chesler, D.A., Goldberg, I.E., Weisskoff, R.M., Poncelet, B.P., Kennedy, D.N., Hoppel, B.E., Cohen, M.S., Turner, R., Cheng, H.M., Brady, T.J., Rosen, B.R., 1992. Dynamic magnetic resonance imaging of human brain activity during primary sensory stimulation. *Proc. Natl. Acad. Sci. U. S. A.* 89, 5675–5679.
- Laufs, H., Kleinschmidt, A., Beyerle, A., Eger, E., Salek-Haddadi, A., Preibisch, C., Kraskow, K., 2003. EEG correlated fMRI of human alpha activity. *NeuroImage* 19, 1463–1476.
- Leopold, D.A., Murayama, Y., Logothetis, N.K., 2003. Very slow activity fluctuations in monkey visual cortex: implications for functional brain imaging. *Cereb. Cortex* 13, 422–433.
- Lowe, M.J., Mock, B.J., Sorenson, J.A., 1998. Functional connectivity in single and multislice echoplanar imaging using resting-state fluctuations. *NeuroImage* 7, 119–132.
- Mazoyer, B., Zago, L., Mellet, E., Bricogne, S., Etard, O., Houde, O., Crivello, F., Joliot, M., Petit, L., Tzourio-Mazoyer, N., 2001. Cortical networks for working memory and executive functions sustain the conscious resting state in man. *Brain Res. Bull.* 54 (3), 287–298.
- Moosmann, M., Ritter, P., Krastel, I., Brink, A., Thees, S., Blakenburg, F., Taskin, B., Obrig, H., Villringer, A., 2003. Correlates of alpha rhythm in functional magnetic resonance imaging and near infrared spectroscopy. *NeuroImage* 20, 145–158.
- Shulman, G.L., Fiez, J.A., Corbetta, M., Buckner, R.L., Miezin, F.M., Raichle, M.E., Petersen, S.E., 1997. Common blood flow changes across visual task: II. Decreases in cerebral cortex. *J. Cogn. Neurosci.*
- Smith, S.M., Jenkinson, M., Woolrich, M., Beckmann, C.F., Behrens, T.E.J., Johansen-Berg, H., Bannister, P.R., De Luca, M., Drobnjak, I., Flitney, D.E., Niazy, R., Saunders, J., Vickers, J., Zhang, Y., De Stefano, N., Brady, J.M., Matthews, P.M., 2004. Advances in functional and structural MR image analysis and implementation as FSL. *NeuroImage* 23 (S1), 208–219.
- Talairach, J., Tournoux, P., 2002. *Co-planar Stereotaxic Atlas of the Human Brain*. Thieme Medical Publishers, New York.
- Ungerleider, L.G., Haxby, J.V., 1994. ‘What’ and ‘where’ in the human brain. *Curr. Opin. Neurobiol.* 4, 157–165.
- Waites, A.B., Stanislavsky, A., Abbott, D.F., Jackson, G.D., 2005. Effect of prior cognitive state on resting state networks measured with functional connectivity. *Hum. Brain Mapp.* 24 (1), 59–68.
- Wise, R.G., Ide, K., Poulin, M.J., Tracey, I., 2004. Resting fluctuations in arterial carbon dioxide induce significant low frequency variations in BOLD signal. *NeuroImage* 21, 1652–1664.
- Xiong, J., Parsons, L.M., Gao, J.H., Fox, P.T., 1999. Interregional connectivity to primary motor cortex revealed using MRI resting state images. *Hum. Brain Mapp.* 8, 151–156.